Genetics and Molecular Research

Cloning and bioinformatic analysis of transcription factor *MYB10* from the red-leaf peach

X.Q. Wang[1], J. Han[1], Y. Wen[1], W.B. Jiang[1], J.G. Fang[1], B.B. Zhang[2] and R.J. Ma[2]

[1]College of Horticulture, Nanjing Agricultural University, Nanjing, China
[2]Institute of Horticulture, Jiangsu Academy of Agricultural Sciences/Jiangsu Key Laboratory of Horticultural Crop Genetic Improvement, Nanjing, China

Corresponding authors: W.B. Jiang / R.J. Ma
E-mail: weibingj@sohu.com / ruijuanm@hotmail.com

Genet. Mol. Res. 15 (4): gmr15048013
Received November 6, 2015
Accepted August 15, 2016
Published October 24, 2016
DOI http://dx.doi.org/10.4238/gmr15048013

ABSTRACT. In higher plants, the transcription factor MYB10 is an important regulator of anthocyanin biosynthesis. In order to study its role in the development of red coloration in peach leaves, the full-length *MYB10* complementary DNA sequence of the red-leaf peach cultivar 'Tsukuba No. 5' (*Prunus persica* f. *atropurpurea*) was successfully cloned using reverse transcription-polymerase chain reaction. The sequence was assigned the GenBank accession No. KP315904. Bioinformatic analysis identified the complete *MYB10* open reading frame, consisting of 678 bp encoding 225 amino acids. The predicted protein has a molecular weight of 26.56 kDa and a theoretical isoelectric point of 8.97. The secondary structure was found to comprise approximately 34.22% alpha helix, 15.11% extended strand, 10.67% beta turn, and 40% random coil. Subcellular analysis indicated

that MYB10 may function in the cytoplasm. Assessment of the amino acid sequence suggested the presence of one serine and two threonine phosphorylation sites. Quantitative real-time polymerase chain reaction revealed that *MYB10* expression positively correlated with anthocyanin content in red-leaf peach, indicating that this transcription factor plays a role in the biosynthesis of this pigment in peach trees.

Key words: Red-leaf peach; *MYB10*; Bioinformatic analysis; Gene expression

INTRODUCTION

The bright purple leaves and high ornamental value of the flowers and fruits of the red-leaf peach (*Prunus persica* f. *atropurpurea*) have drawn this plant increasing attention, resulting in its widespread use in landscaping. Tuan et al. (2015) reported that accumulation of anthocyanin in peach leaves is the main factor responsible for their red or purple coloration, suggesting that such leaf color changes are closely associated with anthocyanin metabolism. Red-leaf peach are colored red early in the growing season, especially during spring, before their anthocyanin content decreases, turning them green in mid-summer and compromising their ornamental value (Xu et al., 2011; Tuan et al., 2015). Therefore, studying the mechanism of anthocyanin metabolism in the red-leaf peach will be helpful in controlling the gain and loss of specific leaf colors.

Previous reports have indicated that anthocyanin biosynthesis is principally controlled by two gene types: structural genes encoding key enzymes in the anthocyanin biosynthesis pathway, such as *CHS*, *CHI*, *F3H*, *F3'H*, *F3'5'H*, *DFR*, *ANS*, and *3GT*, among others; and regulatory genes of the *R2R3-MYB*, *MYC* (*bHLH* family), and *WD40* families that encode transcription factors involved in regulation of structural gene expression (Poovaiah et al., 2016; Shan et al., 2016). These two sets of genes function together to control anthocyanin metabolism in plants (Liu et al., 2013). The functions of *MYB* family genes in the anthocyanin biosynthesis pathway have been well studied in various model plants, such as *Arabidopsis thaliana* (Borevitz et al., 2000), the petunia (Boase et al., 2015), and the gerbera (Shimada et al., 2007). In recent years, most research concerning anthocyanin metabolism has focused on the regulation of transcription factors, especially the interaction between MYB, bHLH, and WD40 proteins (Medina-Puche et al., 2014). These transcription factors regulate biosynthesis of anthocyanin, as shown in *Arabidopsis thaliana* (Palmer et al., 2013), petunias (Boase et al., 2015), and a number of other plants (Dong et al., 2015; Wan et al., 2015). Although the *MYB* family member *MYB10* (GenBank accession No. EU155160) has been isolated from peach fruit, its function has not been closely examined. The red or purple leaves of the red-leaf peach are a major aspect of its ornamental value, which may be improved by elucidating the mechanism behind peach leaf coloration. Moreover, studying the relationship between the regulatory function of MYB in peach leaf anthocyanin biosynthesis and environmental factors would also be of benefit.

In this study, *MYB10* was cloned from the red-leaf peach cultivar 'Tsukuba No. 5', and a bioinformatic analysis of its nucleotide and amino acid sequences was carried out. In addition, its expression pattern in leaves at different growth stages was assessed. The present study provides a theoretical basis for further research regarding the mechanism by which MYB10 regulates anthocyanin metabolism in colored-leaf peaches.

MATERIAL AND METHODS

Plant materials

Samples were collected from the red-leaf peach cultivar 'Tsukuba No. 5', which was grown under normal cultivation conditions at the National Fruit Germplasm Repository of Nanjing, Jiangsu Academy of Agricultural Sciences. After collection, all samples were frozen immediately in liquid nitrogen and stored at -70°C until use.

RNA extraction and complementary DNA (cDNA) synthesis

Total RNA was extracted using the sodium dodecyl sulfate/phenol method (Wang et al., 2004). RNA purity and integrity were assessed by 260/280 nm absorbance ratio and electrophoresis on a 1.0% agarose gel. Total RNA concentration was measured according to absorbance at 260 nm, after genomic DNA had been degraded by DNase I. First-strand cDNA was synthesized from 4 μg DNA-free RNA using a RevertAid First-Strand cDNA Synthesis Kit (Fermentas, Glen Burnie, MD, USA). cDNA was diluted 1:10 before use.

Cloning of the *MYB10* gene

The cDNA thus obtained was used as a template from which to amplify the *MYB10* gene using the following primers: forward, 5'-ATG GAG GGT TAT GAC TTG AGT GTG A-3' and reverse, 5'-TAT TCT TCA TTT GAA TGA TTC CAA GG-3'. Polymerase chain reactions (PCRs) were performed in a final volume of 20 μL, containing 1 μL cDNA, 0.6 μL forward primer, 0.6 μL reverse primer, 0.8 μL deoxynucleotides (10.0 mM), 0.2 μL *Ex Taq*, 2 μL 10X GC buffer, and 14.8 μL double-distilled H_2O. PCR conditions were as follows: 95°C for 5 min, followed by 38 cycles at 95°C for 30 s, 56°C for 1 min, and 72°C for 1 min, with a final extension at 72°C for 10 min. PCR products were detected by electrophoresis on a 1% agarose gel, from which target bands were cut and purified using an AxyPrep DNA Gel Extraction Kit (Axygen Biosciences [Hangzhou] Co., Ltd., Hangzhou, China). The gel-purified PCR products were then subcloned into the pMD18-T vector (TaKaRa, Kusatsu, Japan) and sequenced. The results were compared to the original sequence using DNAMAN (Lynnon Biosoft, San Ramon, CA, USA; Wang et al., 2004), and submitted to the National Center for Biotechnology Information (NCBI; GI No. 1785481).

Bioinformatic analysis

Comparisons of MYB10 nucleotide and deduced amino acid sequences were carried out using online alignment programs (Basic Local Alignment Search Tool, http://blast.ncbi.nlm.nih.gov/Blast.cgi; Zhou et al., 2012). The DNAMAN software package (version 5.2.2) was used for sequence alignments and phylogenetic tree construction. The open reading frame (ORF) was identified using the NCBI's ORF Finder (https://www.ncbi.nlm.nih.gov/orffinder/). The number of amino acids, molecular weight, theoretical isoelectric point (pI), and hydrophobicity of MYB10 were determined with the ProtParam and ProtScale bioinformatic tools provided in ExPASy (http://cn.expasy.org/tools/). Secondary structural elements, including alpha helixes, extended strands, beta turns, and random coils, as well

as the subcellular location of MYB10 were predicted using the SOPMA and PSORT servers via ExPASy. The MYB10 protein sequence was submitted to NPS@ (http://npsa-pbil.ibcp.fr/cgi-bin/npsa) for tertiary structure modeling and NetPhos (http://www.cbs.dtu.dk/services/NetPhos/) for phosphorylation site analysis (Zhou et al., 2012).

Analysis of *MYB10* expression

Quantitative real-time PCR (qPCR) was performed using reaction solutions of 20 μL, each of which contained 10.0 μL SYBR *Premix Ex Taq* (TaKaRa), 0.4 μL forward primer (10 μM), 0.4 μL reverse primer (10 μM), 2 μL cDNA, and 7.2 μL RNase-free water. Reactions were performed in a LightCycler 1.5 instrument (Roche Diagnostics, Mannheim, Germany), and began with a preliminary step at 95°C for 30 s, followed by 40 cycles at 95°C for 5 s and 60°C for 30 s. A template-free control for each primer pair was included on each run. Forward (5'-TGA TTC CAA GGG TCC ACG CTA AAA-3') and reverse (5'-CTG GTC TTG GGT TAG ATG AAG AAC TGC-3') primers were designed based on the cloned *MYB10* sequence. *MYB10* expression was normalized using Ct values resulting from amplification of the peach actin gene with the following primers: forward, 5'-GGT GTG ACG ATG AAG AGT GAT G-3' and reverse, 5'-TGA AGG AGA GGG AAG GTG AAA G-3'. Three technical replicates were performed on each of three biological replicates.

Determination of anthocyanin content

Anthocyanin content was ascertained according to a slight modification of the method described by Ivanova et al. (2011). Briefly, peach leaf samples (1 g) were powdered in liquid nitrogen using a mortar and pestle, and extraction was carried out for 4 h with 10 mL acetone:water mixture (8:2, v/v) containing 0.1% HCl (v/v). Samples were then centrifuged (ST16; Thermo Scientific, Waltham, MA, USA) at 3000 rpm (1006.2 *g*) for 15 min. The supernatants were collected and their final volume increased to 25 mL with distilled water, before being passed through a 0.45-μm polytetrafluoroethylene Iso-Disc filter (Supelco, Bellefonte, PA, USA). The extracts were diluted with a solution of acidified aqueous ethanol (40% ethanol and 0.5% HCl), and absorbance was measured immediately at 540 nm (1-cm optical path). Results are reported as malvidin-3-glucoside equivalents in mg/g fresh mass (FM), and were calculated using the following equation: TA540 nm = A540 nm·16·7d, where A540 nm is absorbance at 540 nm, and d is the dilution.

RESULTS

Cloning and sequencing of the *MYB10* gene

Total RNA of high purity and integrity (Figure 1A) extracted from red peach leaves was used for cDNA synthesis, and the *MYB10* gene was subsequently amplified by PCR (Figure 1B), before being subcloned into the pMD18-T vector and transformed into *Escherichia coli* EH5α cells. Recombinant clones were selected by the "blue-white plaque screening" method, and verified by colony PCR and restriction enzyme digestion, which indicated successful insertion of *MYB10* (678 bp) into the pMD18-T vector and transformation of *E. coli* EH5α cells (Figure 1C and D). Further sequencing of *MYB10* was conducted by Invitrogen Biotech

Co., Ltd. (Shanghai, China), the results of which revealed that the *MYB10* ORF comprises 678 bp in total from the ATG initiation codon to the TGA termination codon, encoding 225 amino acids (Figure 2).

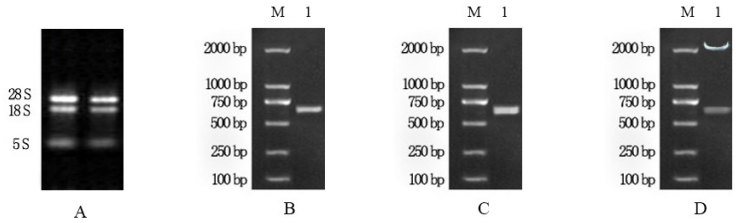

Figure 1. Purified RNA and polymerase chain reaction (PCR) products. **A.** Total RNA extracted from *Prunus persica* f. *atropurpurea* (cultivar 'Tsukuba No. 5'). **B.** Detection of reverse transcription PCR products; *lane 1*: target gene amplification products; *lane M*: molecular marker. **C.** PCR detection of transformed cultures; *lane 1*: positive clones; *lane M*: molecular marker; **D.** Restriction endonuclease digestion of the PMD18-T-PpMYB10 construct; *lane 1*: digestion products; *lane M*: molecular marker.

```
1      atggagggttatgacttgagtgtgagaaaaggagcttggactagagaggaagatgatctt
1       M  E  G  Y  D  L  S  V  R  K  G  A  W  T  R  E  E  D  D  L
61     ctgaggcagtgcattgagaatcaaggtgaaggaaagtggcaccaagttccttacaaagca
21      L  R  Q  C  I  E  N  Q  G  E  G  K  W  H  Q  V  P  Y  K  A
121    gggttgaagaggtgcaggaagagctgtagactaaggtgggtgaactatttgaagccaaat
41      G  L  K  R  C  R  K  S  C  R  L  R  W  V  N  Y  L  K  P  N
181    atcaagaaaggagactttgcagaggatgaagtagatctaataattaggcttcacaagctt
61      I  K  K  G  D  F  A  E  D  E  V  D  L  I  I  R  L  H  K  L
241    ctaggaaacaggtggtcattgattgctcgaagacttccaggaaggactgcgaataatgtg
81      L  G  N  R  W  S  L  I  A  R  R  L  P  G  R  T  A  N  N  V
301    aaaaattactggaacacccgattgcggacggattattgcatgaaaaagataaaagacaaa
101     K  N  Y  W  N  T  R  L  R  T  D  Y  C  M  K  K  I  K  D  K
361    ccccaagaaacaataaagaccatcataataaggccacaaccaagaagattcaccaaaagt
121     P  Q  E  T  I  K  T  I  I  I  R  P  Q  P  R  R  F  T  K  S
421    tcaaattgtttgagttttaaagaaccaattttggaccatactcaacgtgattggtgggag
141     S  N  C  L  S  F  K  E  P  I  L  D  H  T  Q  R  D  W  W  E
481    acctttttagatgacaaggatgctactgaaagagctacaggttctggtcttgggttagat
161     T  F  L  D  D  K  D  A  T  E  R  A  T  G  S  G  L  G  L  D
541    gaagaactgctcgcaagtttttgggttgatgatgatatgccacaatcgacaagaaaatgc
181     E  E  L  L  A  S  F  W  V  D  D  D  M  P  Q  S  T  R  K  C
601    atcaatttttctgaaggactaagtagaggtgatttctcttttagcgtggacctttggaat
201     I  N  F  S  E  G  L  S  R  G  D  F  S  F  S  V  D  L  W  N
661    cattcaaaagaagaatag
221     H  S  K  E  E  *
```

Figure 2. Full-length MYB10 nucleotide and putative amino acid sequences.

Multiple-sequence alignment and phylogenetic analysis

The deduced peach MYB10 amino acid sequence and 12 closely related homologous protein sequences, including those of *Prunus persica* (ABX79945.1), *Prunus dulcis* (ABX79944.1), *Prunus salicina* (ABX79946.1), *Prunus armeniaca* (ABX71490.1), *Prunus avium* (ABX71493.1), *Prunus mume* (XP_008244325.1), *Malus domestica* (ABB84753.1), *Pyrus pyrifolia* (ABX71488.1), *Actinidia chinensis* (AHY00342.1), *Eriobotrya japonica* (ABX71484.1), *Fragaria* x *ananassa* (ABX79947.1), and *Vitis vinifera* (BAP39802.1), were aligned with DNAMAN version 5.2.2. This alignment was then used to create a phylogenetic tree using the neighbor-joining method and standard parameters. Homology between the various plant MYB10 proteins ranged from 47 to 97%. The red-leaf peach MYB10 sequence

demonstrated the highest degrees of homology with *P. persica* (97%) and *P. dulcis* (94%; Figure 3), and phylogenetic analysis showed it to be most closely related to those of these species (Figure 4). The phylogenetic tree indicated that the MYB10 protein of the red-leaf peach shares a close evolutionary relationship with those of rosaceous plants.

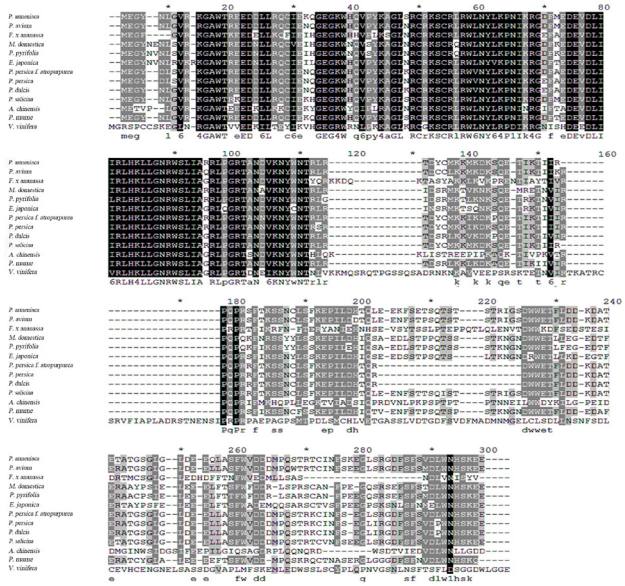

Figure 3. Assessment of homology between the amino acid sequence of MYB10 from *Prunus persica* f. *atropurpurea* and those of other plant species.

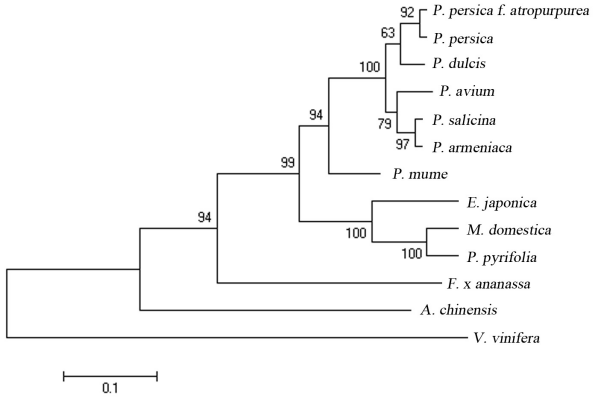

Figure 4. Phylogenetic analysis of MYB10 amino acid sequences from *Prunus persica* f. *atropurpurea* and other plant species.

Physical and chemical properties of the red-leaf peach MYB10 protein

The physical and chemical properties of MYB10, including its amino acid number, molecular weight, theoretical pI, and hydrophobicity were analyzed using the ExPASy

bioinformatic web resource. Red-leaf peach MYB10 was found to be an unstable hydrophilic protein with a predicted molecular weight of 26.56 kDa, a theoretical pI of 8.97, a theoretical half-life of 30 h, and an instability index value of 44.52 (values greater than 40 signify instability). Its amino acid composition is shown in Table 1. Forty-one (18.2%) positively charged (Arg and Lys) and 35 (15.5%) negatively charged amino acids (Asp and Glu) were present. Red-leaf peach MYB10 was shown to be a hydrophilic protein, with the most hydrophobic residue at position 77 (Leu) and the most hydrophilic at position 156 (Arg; Figure 5).

Table 1. Amino acid contents of MYB10.

Composition of amino acids	Number	Percentage (%)	Composition of amino acids	Number	Percentage (%)
Ala (A)	8	3.6	Leu (L)	22	9.8
Arg (R)	21	9.3	Lys (K)	20	8.9
Asn (N)	11	4.9	Met (M)	3	1.3
Asp (D)	19	8.4	Phe (F)	8	3.6
Cys (C)	6	2.7	Pro (P)	8	3.6
Gln (Q)	7	3.1	Ser (S)	14	6.2
Glu (E)	16	7.1	Thr (T)	12	5.3
Gly (G)	13	5.8	Trp (W)	9	4.0
His (H)	4	1.8	Tyr (Y)	5	2.2
Ile (I)	12	5.3	Val (V)	7	3.1

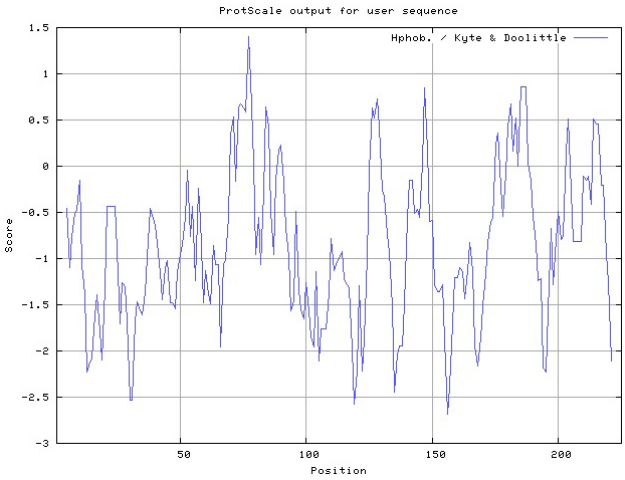

Figure 5. Analysis of the hydrophobicity of MYB10.

Protein structure analysis and subcellular localization

The MYB10 protein from the red-leaf peach was observed to have no transmembrane domain, transmembrane helix, or signal peptide (Figure 6). Secondary structure prediction found it to be 34.22% alpha helix, 10.67% beta turn, 40% random coil, and 15.11% extended strand (Figure 7). Tertiary structure modeling showed that a large proportion of this MYB10 protein is made up of alpha-helixes and random coils, with a small portion forming beta-turns and extended strands (Figure 8). Analysis using the NetPhos 2.0 server identified one serine and two threonine phosphorylation sites, indicating that the phosphorylated MYB10 protein is

involved in the regulation of anthocyanin biosynthesis in the red-leaf peach (Figure 9). Assessment of subcellular localization suggested that MYB10 is present in the cytoplasm (Table 2).

Table 2. Subcellular localization prediction of protein MYB10 from *Prunus persica* f. *atropurpurea*.

MYB10	Probability of occurrence (%)
Cytoplasmic	45
Microbody	38.4
Mitochondrial matrix space	10
Lysosome	10

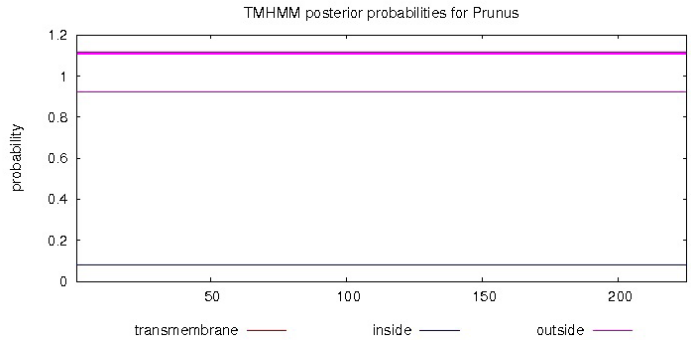

Figure 6. Analysis of the presence of transmembrane domains in MYB10.

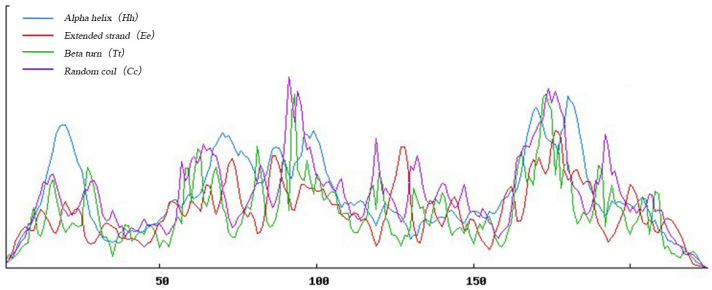

Figure 7. Prediction of MYB10 secondary structure.

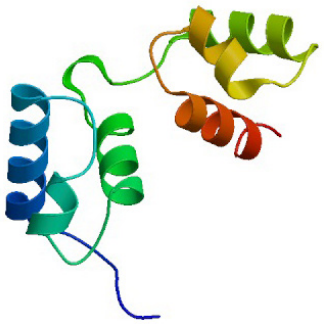

Figure 8. Prediction of MYB10 tertiary structure.

Figure 9. Analysis of phosphorylation sites in MYB10.

Changes in anthocyanin content and *MYB10* expression

The anthocyanin content of red-leaf peach during the growing season exhibited a 'V'-shaped trend, peaking at 3.935 mg/g FM in May, and then dropping sharply to its lowest level of 1.386 mg/g FM in July, before increasing in August and September (Figure 10). This shows that anthocyanin content correlates highly with the pattern of color change observed in red-leaf peach (Figure 11). Moreover, qPCR revealed that *MYB10* expression varied in a manner similar to that of anthocyanin content, also showing a 'V'-shaped pattern (Figure 12). These data indicate that the *MYB10* gene might be involved in the regulation of anthocyanin metabolism.

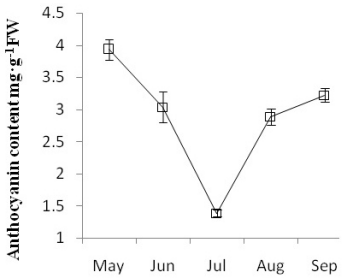

Figure 10. *Prunus persica* f. *atropurpurea* leaves on five different months.

Figure 11. Total anthocyanin content in leaves of the peach *Prunus persica* f. *atropurpurea*.

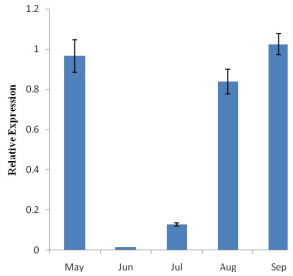

Figure 12. *MYB10* expression in leaves of the peach *Prunus persica* f. *atropurpurea* on five different months.

DISCUSSION

MYB proteins have developed increasingly diverse functions over the course of plant evolution. However, the MYB transcription factor-regulatory mechanism remains far from clear. For example, most *MYB* genes positively regulate anthocyanin accumulation (Chagné et al., 2013; Li et al., 2014; Lin-Wang et al., 2014), although a small number function as negative regulators (Aharoni et al., 2001; Yang et al., 2015). The transcription factor R2R3-MYB has many regulatory modes in anthocyanin biosynthesis (Wang et al., 2004; Yang et al., 2015). In the grapevine, *VvMYB5a* is mainly expressed during early stages in the development of skin, flesh, and seeds, whereas *Vvmyb5A1* is only expressed in grape skins (Deluc et al., 2006; Shan et al., 2016). In certain plants, MYB proteins regulate anthocyanin biosynthesis by interacting with bHLH proteins, a mechanism that has been widely studied in petunias (Quattrocchio et al., 2006; Boase et al., 2015), snapdragons (Schwinn et al., 2006; Butelli et al., 2008), and maize (Grotewold et al., 1998; Dong et al., 2015). In *Arabidopsis thaliana*, *TT2*, *TT8*, and *TTG1* encode an R2R3-MYB domain protein, a bHLH transcription factor, and a WD40-repeat-containing protein, respectively, and their tripartite interaction regulates expression of flavonoid structural genes (Nesi et al., 2001; Starkevič et al., 2015). In this study, expression of the *MYB10* gene was high, and correlated with elevated anthocyanin content in red-leaf peach (Figures 11 and 12). This is consistent with the results of previous studies (Ban et al., 2007; Wan et al., 2015; Zhang et al., 2016), in which *MYB*-like genes have been found to positively regulate the synthesis and accumulation of anthocyanin.

In the present study, we cloned the gene encoding the MYB10 transcription factor from red-leaf peach and submitted its sequence to GenBank (Accession No. KP315904). Bioinformatic analysis showed that its ORF was 678 bp long, encoding a 225-amino acid protein with a predicted molecular weight of 26.56 kDa and a theoretical pI of 8.97. Comparison with homologous proteins revealed that red-leaf peach MYB10 has a close evolutionary relationship with those of rosaceous plants. Structural analysis showed it to be an intrinsic membrane protein located in the cytoplasm, with one serine and two threonine phosphorylation sites. Its secondary structure comprised 34.22% alpha helix, 10.67% beta turn, 40% random coil, and 15.11% extended strand. The composition and distribution of these secondary structural elements are visually presented in the tertiary structure model.

Certain studies of factors regulating anthocyanin biosynthesis have demonstrated that the protein AN2 plays an important role in determining petunia coloration (Boase et al., 2015), and that *AtPAP1* and *AtPAP2* regulate anthocyanin accumulation in *Arabidopsis thaliana* stems and leaves (Borevitz et al., 2000; Li et al., 2014). In the grapevine, *VvMyb*A controls anthocyanin biosynthesis by modulating *UFGT* expression (Kobayashi et al., 2002; Dong et al., 2015). In the current study, *MYB10* expression reflected the anthocyanin content of red-leaf peach, both exhibiting high levels in May that dropped sharply in June and July, before recovering in August and September. We also observed that changes in *MYB10* expression preceded those in anthocyanin content; for example, *MYB10* transcription dropped to its lowest level in June, whereas anthocyanin content was lowest in July (Figures 11 and 12). This indicates that *MYB10* may positively regulate biosynthesis of anthocyanin, and play an important role in its accumulation in red-leaf peach. This study will surely facilitate further research concerning the interaction between MYB, bHLH, and WD40 proteins as a mechanism regulating anthocyanin biosynthesis, and provides a theoretical basis for transgenic red-leaf peach breeding.

Conflicts of interest

The authors declare no conflict of interest.

ACKNOWLEDGMENTS

Research supported by the National Natural Science Foundation of China (#31101517) and the Science and Technology Innovation Foundation of Nanjing Agricultural University Young Teachers (#KJ09010).

REFERENCES

Aharoni A, De Vos CH, Wein M, Sun Z, et al. (2001). The strawberry *FaMYB1* transcription factor suppresses anthocyanin and flavonol accumulation in transgenic tobacco. *Plant J.* 28: 319-332. http://dx.doi.org/10.1046/j.1365-313X.2001.01154.x

Ban Y, Honda C, Hatsuyama Y, Igarashi M, et al. (2007). Isolation and functional analysis of a MYB transcription factor gene that is a key regulator for the development of red coloration in apple skin. *Plant Cell Physiol.* 48: 958-970. http://dx.doi.org/10.1093/pcp/pcm066

Boase MR, Brendolise C, Wang L, Ngo H, et al. (2015). Failure to launch: the self-regulating *Md-MYB10* $_{R6}$ gene from apple is active in flowers but not leaves of *Petunia. Plant Cell Rep.* 34: 1817-1823. http://dx.doi.org/10.1007/s00299-015-1827-4

Borevitz JO, Xia Y, Blount J, Dixon RA, et al. (2000). Activation tagging identifies a conserved MYB regulator of phenylpropanoid biosynthesis. *Plant Cell* 12: 2383-2394. http://dx.doi.org/10.1105/tpc.12.12.2383

Butelli E, Titta L, Giorgio M, Mock HP, et al. (2008). Enrichment of tomato fruit with health-promoting anthocyanins by expression of select transcription factors. *Nat. Biotechnol.* 26: 1301-1308. http://dx.doi.org/10.1038/nbt.1506

Chagné D, Lin-Wang K, Espley RV, Volz RK, et al. (2013). An ancient duplication of apple MYB transcription factors is responsible for novel red fruit-flesh phenotypes. *Plant Physiol.* 161: 225-239. http://dx.doi.org/10.1104/pp.112.206771

Deluc L, Barrieu F, Marchive C, Lauvergeat V, et al. (2006). Characterization of a grapevine R2R3-MYB transcription factor that regulates the phenylpropanoid pathway. *Plant Physiol.* 140: 499-511. http://dx.doi.org/10.1104/pp.105.067231

Dong ZD, Chen J, Li T, Chen F, et al. (2015). Molecular survey of *Tamyb10-1* genes and their association with grain colour and germinability in Chinese wheat and *Aegilops tauschii. J. Genet.* 94: 453-459. http://dx.doi.org/10.1007/s12041-015-0559-0

Grotewold E, Chamberlin M, Snook M, Siame B, et al. (1998). Engineering secondary metabolism in maize cells by ectopic expression of transcription factors. *Plant Cell* 10: 721-740.

Ivanova V, Stefova M, Vojnoski B, Dornyei A, et al. (2011). Identification of polyphenolic compounds in red and white grape varieties grown in R. Macedonia and changes of their content during ripening. *Food Res. Int.* 44: 2851-2860. http://dx.doi.org/10.1016/j.foodres.2011.06.046

Kobayashi S, Ishimaru M, Hiraoka K and Honda C (2002). *Myb*-related genes of the Kyoho grape (*Vitis labruscana*) regulate anthocyanin biosynthesis. *Planta* 215: 924-933. http://dx.doi.org/10.1007/s00425-002-0830-5

Li P, Zhang Y, Einhorn TC and Cheng L (2014). Comparison of phenolic metabolism and primary metabolism between green 'Anjou' pear and its bud mutation, red 'Anjou'. *Physiol. Plant.* 150: 339-354. http://dx.doi.org/10.1111/ppl.12105

Lin-Wang K, McGhie TK, Wang M, Liu Y, et al. (2014). Engineering the anthocyanin regulatory complex of strawberry (*Fragaria vesca*). *Front. Plant Sci.* 5: 651. http://dx.doi.org/10.3389/fpls.2014.00651

Liu YZ, Luo WL, Huang CH, Chen LK, et al. (2013). Characterization of the regulatory dene *hrd1(t)* involved in anthocyanin biosynthesis. *Zhongguo Nong Ye Ke Xue* 46: 3955-3964.

Medina-Puche L, Cumplido-Laso G, Amil-Ruiz F, Hoffmann T, et al. (2014). *MYB10* plays a major role in the regulation of flavonoid/phenylpropanoid metabolism during ripening of *Fragaria* x *ananassa* fruits. *J. Exp. Bot.* 65: 401-417. http://dx.doi.org/10.1093/jxb/ert377

Nesi N, Jond C, Debeaujon I, Caboche M, et al. (2001). The *Arabidopsis TT2* gene encodes an R2R3 MYB domain protein that acts as a key determinant for proanthocyanidin accumulation in developing seed. *Plant Cell* 13: 2099-2114.

Palmer CM, Hindt MN, Schmidt H, Clemens S, et al. (2013). *MYB10* and *MYB72* are required for growth under iron-limiting conditions. *PLoS Genet.* 9: e1003953. http://dx.doi.org/10.1371/journal.pgen.1003953

Poovaiah CR, Bewg WP, Lan W, Ralph J, et al. (2016). Sugarcane transgenics expressing MYB transcription factors show improved glucose release. *Biotechnol. Biofuels* 9: 143. http://dx.doi.org/10.1186/s13068-016-0559-1

Quattrocchio F, Verweij W, Kroon A, Spelt C, et al. (2006). PH4 of *Petunia* is an R2R3 MYB protein that activates vacuolar acidification through interactions with basic-helix-loop-helix transcription factors of the anthocyanin pathway. *Plant Cell* 18: 1274-1291. http://dx.doi.org/10.1105/tpc.105.034041

Schwinn K, Venail J, Shang Y, Mackay S, et al. (2006). A small family of *MYB*-regulatory genes controls floral pigmentation intensity and patterning in the genus *Antirrhinum*. *Plant Cell* 18: 831-851. http://dx.doi.org/10.1105/tpc.105.039255

Shan T, Rong W, Xu H, Du L, et al. (2016). The wheat R2R3-MYB transcription factor TaRIM1 participates in resistance response against the pathogen *Rhizoctonia cerealis* infection through regulating defense genes. *Sci. Rep.* 6: 28777. http://dx.doi.org/10.1038/srep28777

Shimada S, Otsuki H and Sakuta M (2007). Transcriptional control of anthocyanin biosynthetic genes in the Caryophyllales. *J. Exp. Bot.* 58: 957-967. http://dx.doi.org/10.1093/jxb/erl256

Starkevič P, Paukštytė J, Kazanavičiūtė V, Denkovskienė E, et al. (2015). Expression and anthocyanin biosynthesis-modulating potential of sweet cherry (*Prunus avium* L.) *MYB10* and *bHLH* genes. *PLoS One* 10: e0126991. http://dx.doi.org/10.1371/journal.pone.0126991

Tuan PA, Bai S, Yaegaki H, Tamura T, et al. (2015). The crucial role of *PpMYB10.1* in anthocyanin accumulation in peach and relationships between its allelic type and skin color phenotype. *BMC Plant Biol.* 15: 280. http://dx.doi.org/10.1186/s12870-015-0664-5

Wan H, Zhang J, Song T, Tian J, et al. (2015). Promotion of flavonoid biosynthesis in leaves and calli of ornamental crabapple (*Malus* sp.) by high carbon to nitrogen ratios. *Front. Plant Sci.* 6: 673. http://dx.doi.org/10.3389/fpls.2015.00673

Wang ZW, Qu SC, Zhang Z and Zhang JY (2004). A fast method for total RNA extraction from the tissue culture material of *Malus* sp. *Guoshu Xuebao* 21: 385-387.

Xu LL, Jiang WB, Han J, Weng ML, et al. (2011). Effects of foliage spray of KH_2PO_4 and sucrose solution on changes of pigments and net photosynthetic rate in leaves of red-leaf peach in early summer. *Sci. Silvae Sin.* 47: 170-174.

Yang YN, Yao GF, Zheng D, Zhang SL, et al. (2015). Expression differences of anthocyanin biosynthesis genes reveal regulation patterns for red pear coloration. *Plant Cell Rep.* 34: 189-198. http://dx.doi.org/10.1007/s00299-014-1698-0

Zhang YZ, Xu SZ, Cheng YW, Ya HY, et al. (2016). Transcriptome analysis and anthocyanin-related genes in red leaf lettuce. *Genet. Mol. Res.* 15: doi: 10.4238/gmr.15017023. http://dx.doi.org/10.4238/gmr.15017023

Zhou MJ, Hu SL, Cao Y, Lu XQ, et al. (2012). Cloning and bioinformation analysis of *C3H* gene in *Neosinocalamus affinis*. *Bull. Bot. Res.* 32: 38-46.